







frequencies in OWT's operation. However, no commonly acceptable approach exists for linearization of the nonlinear soil spring models so far. If the loading time history data are given, nonlinear dynamic analysis can be carried out. However, loading and unloading curves for the soil response must be available even in these cases.

In this study, the nonlinear soil springs are linearized considering the equivalent load amplitude which is obtained mainly from the thrust force time history data by a coupled analysis program such as FAST or HAWC2 (see Fig. 3). The thrust forces, which are main external loads in OWTs, are determined at the rated wind speed where high thrust forces with significant fluctuations are generated. Existing OWTs are designed with rated rotor speeds of, for example, 7-14 rounds per minute (RPM) leading to blade-passing speeds of 21-42 RPM. For new generations of OWTs, the cut-in rotational speed is reduced to extract more wind energy. Hence, the gap between the maximum allowable 1P frequency and the minimum allowable 3P frequency is closing. Because of this, soft-stiff design becomes more difficult and may require an enhanced modern control strategy such as variable speed control with the speed exclusive zone algorithm (Licari 2013).

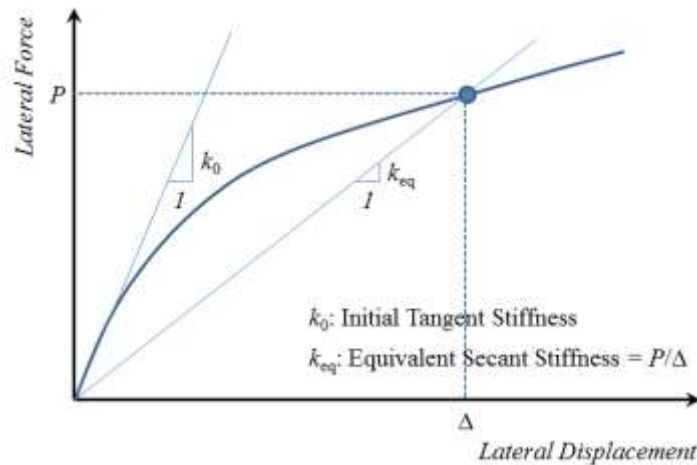
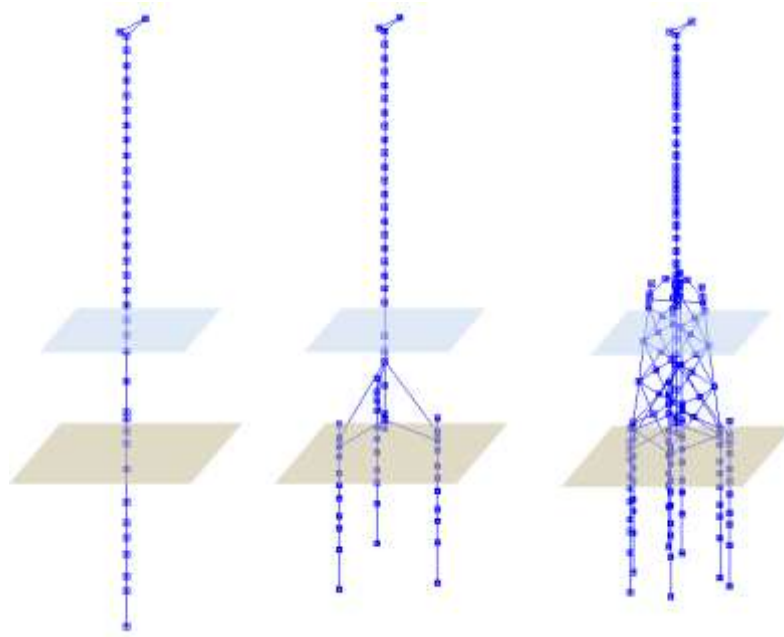


Fig. 3 Equivalent secant stiffness of nonlinear soil spring

### 3. EXAMPLE STUDY

#### 3.1 Example Wind Turbine Model

The NREL 5 MW wind turbines, placed on a monopile, tripod and jacket substructure, are utilized in this study. The soil properties including statistical data are obtained from cone penetration tests (CPTs) carried out in the south-west coastal region of Korea. The pre-pile method is considered with vertical piles (not battered ones) for the cases of tripod- and jacket-type substructures as shown in Fig. 4. Details of the model are listed in Table 1. The rotor, hub and nacelle are simplified as a lumped mass at the top of the tower, i.e. rotor and hub masses are lumped at the mass center of hub and nacelle mass is placed at the mass center of nacelle.



(a) Monopile                      (b) Tripod                      (c) Jacket

Fig. 4 Wind turbine model with jacket (not scaled)

Table 1. Specification of OWT models

(a) Tower

|                               |                         |
|-------------------------------|-------------------------|
| Hub height                    | 90 m                    |
| TP height                     | 20 m                    |
| Tower thickness(top/bottom)   | 20 mm                   |
| Tower diameter(top/bottom)    | 3.87 m/ 6 m             |
| Top mass (blades+hub+nacelle) | 251.2 ton               |
| Density                       | 7,850 kg/m <sup>3</sup> |

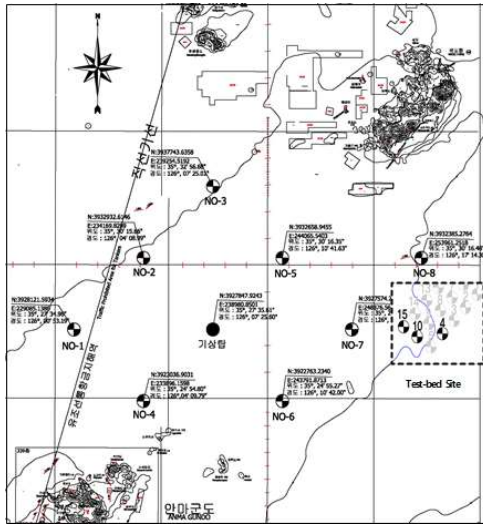
(b) Substructures

|                   | Monopile | Tripod | Jacket |
|-------------------|----------|--------|--------|
| TP height         | 15.4 m   | 16.0 m | 25.5 m |
| Pile diameter     | 5.7 m    | 2.5 m  | 1.45 m |
| Pile thickness    | 70 mm    | 40 mm  | 40 mm  |
| Penetration Depth | 30 m     | 40 m   | 40 m   |

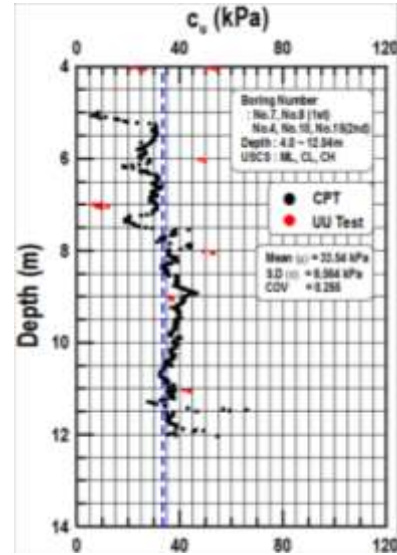
### 3.2 Uncertainties in Soil Properties

The first large-scale offshore wind farm project was initiated to develop the core technologies including planning, design, manufacturing, installation and O&M (operation and management) for offshore wind farms in Korea. The target site was situated in the south-west coastal region, and several soil investigation works such as

SPT and CPT were carried out to obtain the soil condition. Typical CPT data are shown in Fig. 5 and the statistical properties of each soil layer are summarized in Table 2. The values are mean values obtained from CPT and the coefficients of variation (COVs) are found to be 0.1 for the unit weight, 0.225 for the cohesion, and 0.062 for the internal angle of friction.



(a) Target site for offshore wind farm



(b) CPT data for BH-7

Fig. 5. Target site and CPT data for offshore wind farm in Korea

Table 2. Characteristic values for soil layers at the target site

| Soil layers |    | Depth (m) | Unit weight               |     | Cohesion   |       | Angle of internal friction |       |
|-------------|----|-----------|---------------------------|-----|------------|-------|----------------------------|-------|
|             |    |           | Mean (kN/m <sup>3</sup> ) | COV | Mean (kPa) | COV   | Mean (°)                   | COV   |
| Silt        | CH | 0–5.0     | 17.0                      | 0.1 | 20.00      | 0.225 | -                          | 0.062 |
|             | CL | 5.0–12.3  | 18.0                      |     | 33.54      |       | -                          |       |
| Sand        | SM | 12.3–23.0 | 19.0                      |     | 16.63      |       | 31.59                      |       |
| Silt        | CL | 23.0–30.0 | 18.0                      |     | 60.00      |       | -                          |       |

### 3.3 Numerical Analysis Results

Figure 6 shows one of the thrust force time histories obtained from FAST with the near-rated wind speed of 12.0 m/s without PSI effects for different normal turbulence models (NTM), i.e. NTM-A, B, and C. For a given wind speed, the statistical properties of the thrust forces (including the mean and standard deviation) are assumed to be the same whether the substructure is fixed at mud-line or the PSI model is introduced. As mentioned before, the equivalent load amplitude is decided using the standard deviation of the thrust force, and the nonlinear soil springs are linearized under the equivalent load amplitude at the top of the tower (i.e. at hub height). For simplicity, wave loading is not considered. It can easily be included in the analysis, but it will not be significant for this study.

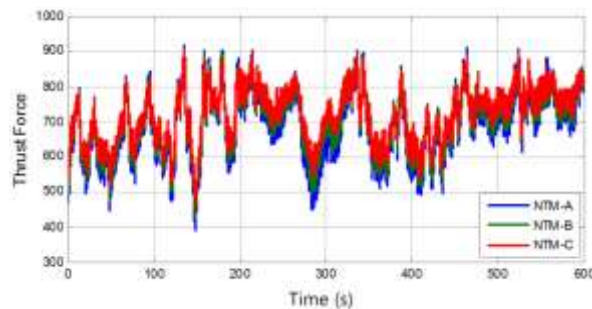


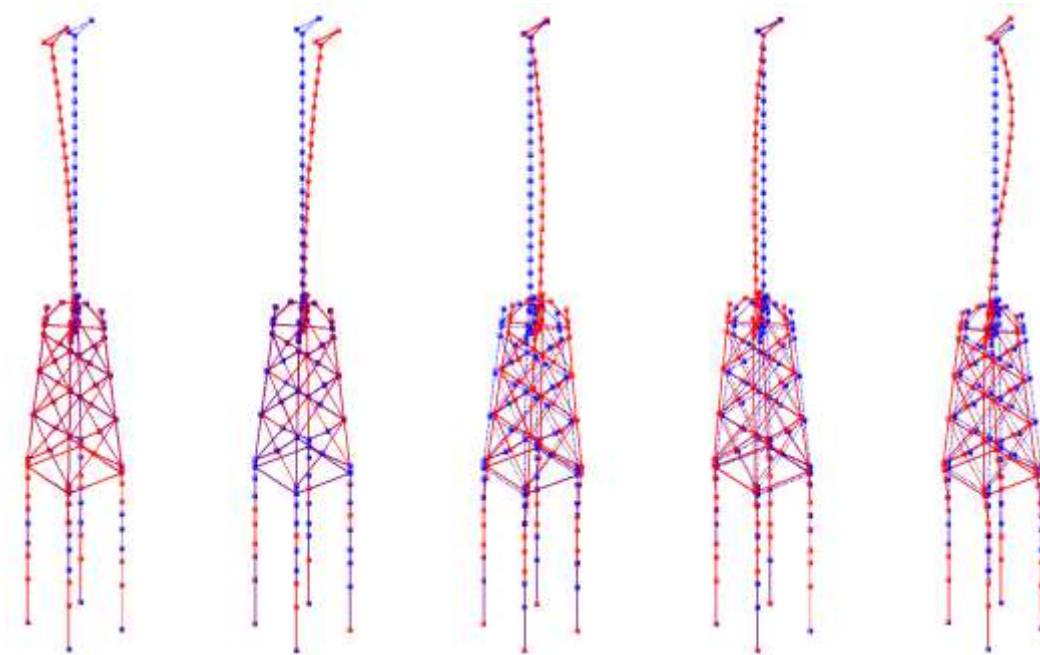
Fig. 6. Thrust force time history data under rated wind speed

Fig. 7 shows the mode shapes and natural frequencies calculated with the linearized soil springs obtained at the rated wind speed. The effect of the equivalent load amplitude can be included in the linearized soil spring stiffness; i.e. the secant stiffness will become smaller as the equivalent load amplitude becomes larger, and vice versa. To investigate the effect of equivalent load amplitude, the first natural frequency is compared with respect to the equivalent load amplitude of thrust force in Figs. 8 and 9. As expected, the natural frequency tends to become smaller as the equivalent load amplitude of the thrust force increases. For each loading conditions, one thousand samples are randomly generated considering the mean values and COVs of the soil properties. The histogram for the representative four cases are shown in Fig. 8 and the mean values plus/minus three standard deviation for all cases are shown in Fig. 9.

The mean value is gradually reduced from 0.2512 Hz to 0.2493 Hz, 0.2479 Hz, and so on for the case of monopile-supported OWT while that is from 0.2690 Hz to 0.2687 Hz, 0.2685 Hz, ... and from 0.3240 Hz to 0.3230 Hz, 0.3223 Hz, ... for tripod- and jacket-supported OWTs, respectively. When the equivalent load amplitude is increased from 10 kN to 210 kN, the mean value of the natural frequency is decreased as mentioned before and the reduction ratios for three different supporting structures are 4.86 %, 0.59 % and 1.82 % for monopile, tripod and jacket supported OWTs, respectively, as indicated in Table OO. The effect of equivalent load amplitude is more significant for the monopile-supported OWTs while it is less significant for the tripod case, which means that the nonlinear behavior of soil media affects more significantly for monopile case. Even though it is certainly true that the natural frequency is reduced as the equivalent load amplitude is increased, the change is small and almost negligible from a practical point of view at least for the cases of multi-member lattice-type substructures like tripods and jackets.

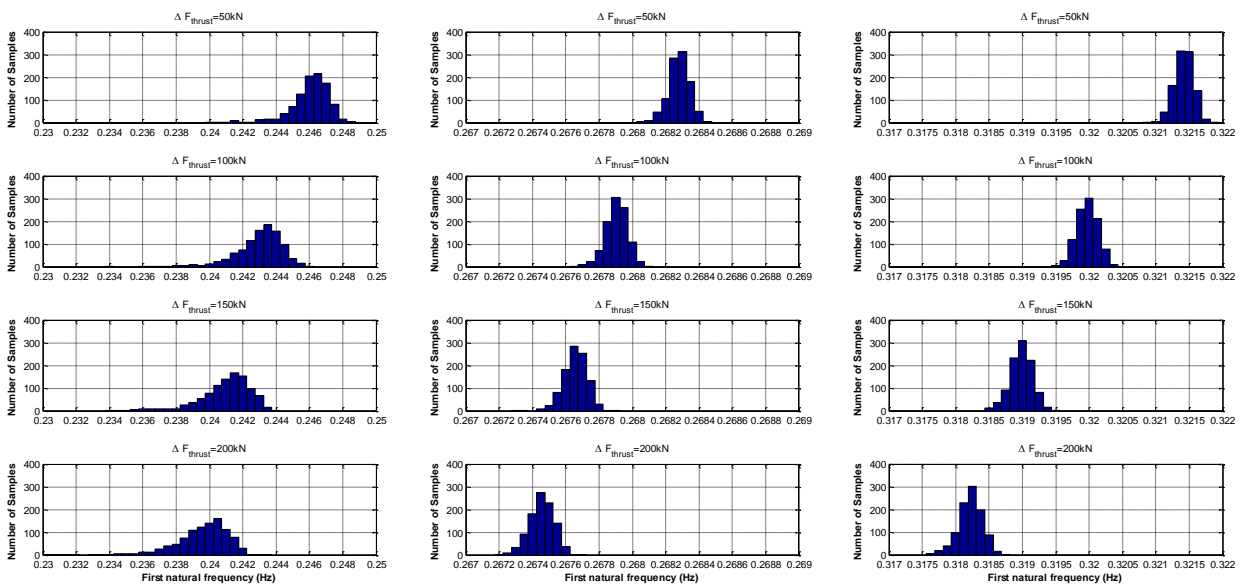
The first natural frequencies which are calculated considering the PSI effects are also compared with those without PSI effects, i.e. fixed and hinged cases in Table 3. It can be found that the natural frequency is reduced as amount of 12.3 % for the case of monopile-supported OWT while they are less than 1.4 % and 2.7 % for the cases of tripod and jacket substructures, respectively, by introducing nonlinear PSI effects. This means that the first natural frequency can be reasonably estimated by neglecting the

PSI effect in the cases of multi-member lattice-type substructures when the soil properties are not fully known or completely unknown in the preliminary design stage.



$$f_1 = 0.3382\text{Hz} \quad f_2 = 0.3393\text{Hz} \quad f_3 = 2.4639\text{Hz} \quad f_4 = 2.7159\text{Hz} \quad f_5 = 4.8703\text{Hz}$$

Fig. 7 Lower 5 modes for the 5 MW example wind turbine model



(a) Monopile-type OWTs

(b) Tripod-type OWTs

(c) Jacket-type OWTs

Fig. 8 Histogram of first natural frequencies from 1000 samples



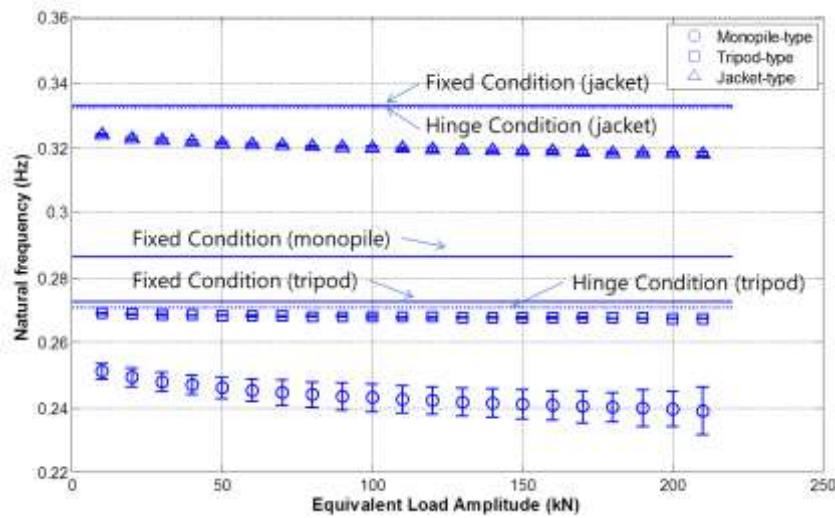


Fig. 9  $\mu$  and  $\mu \pm 3\sigma$  of first natural frequencies with different equivalent load amplitudes

Table 3. Natural frequencies for various conditions

| Case    |  | Monopile | Tripod | Jacket |
|---------|--|----------|--------|--------|
| Fixed   | $f_1^{fixed}$ (Hz)                     | 0.2864   | 0.2728 | 0.3329 |
| Hinged  | $f_1^{hinged}$ (Hz)                    | -        | 0.271  | 0.3322 |
|         | $1 - f_1^{hinged} / f_1^{fixed}$ (%)   | -        | 0.66%  | 0.21%  |
| P=10kN  | $f_1^{P=10kN}$ (Hz)                    | 0.2512   | 0.2690 | 0.3240 |
|         | $1 - f_1^{P=10kN} / f_1^{fixed}$ (%)   | 12.29%   | 1.39%  | 2.67%  |
| P=210kN | $f_1^{P=210kN}$ (Hz)                   | 0.2390   | 0.2674 | 0.3181 |
|         | $1 - f_1^{P=210kN} / f_1^{P=10kN}$ (%) | 4.86%    | 0.59%  | 1.82%  |

#### 4. CONCLUDING REMARKS

From the numerical analysis of the NREL 5 MW wind turbine models supported by monopole, tripod and jacket substructures, the PSI effects on the natural frequencies are investigated and it is found that the uncertainties of soil properties can affect the first natural frequency distributions under several conditions with different equivalent loading amplitudes. The stiffness of soil springs decreases as the equivalent loading amplitude increases, which implies a reduction of the natural frequency. However, the reduction is small (less than 2%) and may thus be negligible from a practical point of view for the cases of tripod- and jacket-supported OWTs.

One interesting observation is that the natural frequency is getting more significantly affected by the equivalent load amplitude in the case of the monopile-type OWT. And also it is observed that the variability of natural frequency is larger in the cases of the monopile-type OWT. It means that the PSI effects on the natural frequency

of tripod- and jacket-supported OWTs are less significant than that of a monopile-type OWT. In other words, the jacket-supported OWT is more robust regarding consistency of the natural frequency under different equivalent load amplitudes and uncertain soil conditions. Of course, the optimal water depths for monopile and jacket foundations are quite different; i.e. in shallow water less than 30 m deep, the monopile foundation can be more efficiently utilized, while in intermediate water depths of 25–50 m, the jacket foundation is attractive. However, in water depths between 20 and 30 m, the jacket and monopile foundations are still competitive with each other and both of them can be applicable depending on site conditions such as soil conditions. Economic feasibility to reduce the cost of energy will be the first index for deciding which foundation type to use within this range.

## ACKNOWLEDGEMENTS

This work was supported by the Korea Institute of Energy Technology Evaluation and Planning (KETEP) grant (20123030020110) and the international network programme “Reliability-based design of offshore wind turbines with focus on load estimation and dynamic soil–structure interaction” supported by the Danish Agency for Science Technology and Innovation Framework Grant No. 1370-00125A. The authors would like to express their appreciation for the financial support.

## REFERENCES

- Alexander, NA and Bhattacharya, S (2011), “The Dynamics of Monopile-Supported Wind Turbines in Nonlinear Soil.” *Proceedings of the 8th International Conference on Structural Dynamics, EURO DYN 2011*, Leuven, Belgium, 4-6 July 2011, 3416-3422.
- API (2005) *Recommended Practice for Planning, Design and Constructing Fixed Offshore Platforms-Working Stress Design*. American Petroleum Institute Publishing Service, Washington D.C., 1-263.
- Bisoi, S, and Haldar, S (2014). “Dynamic Analysis of Offshore Wind Turbine in Clay Considering Soil-Monopile-Tower Interaction.” *Soil Dynamics and Earthquake Engineering*, 63, 19-35.
- Carswell, W. (2012) *Probabilistic Analysis of Offshore Wind Turbine Soil-Structure Interaction*. MSc Thesis, University of Massachusetts, Amherst.
- Carswell, W, Arwade, SR, Myers, AT, and Hajjar, JF (2014). *Safety, Reliability, Risk and Life-Cycle Performance of Structures and Infrastructures*, CRC Press, 223-229.
- Evans, L.T. Jr. and Duncan, J.M. (1982) *Simplified Analysis of Laterally Loaded Piles*. Report UCB/GT/82-04, University of California, Berkley.
- EWEA (2013) *Deep water – The next step for offshore wind energy*, A report by the European Wind Energy Association.
- Martinez-Chaluisant, V. (2011). *Static and Dynamic Response of Monopiles for Offshore Wind Turbines*, University of Wisconsin-Madison
- Licari, J. (2013) *Control of a variable-speed wind turbine*, PhD Thesis, Institute of Energy, Cardiff University.

- Pradhan, DL (2012) *Development of P-Y Curves for Monopiles in Clay using Finite Element Model Plaxis 3D Foundation*, Norwegian University of Science and Technology.
- Song, B, Huang, FT, and Li, KW(2014). "Pile-soil Interaction Impact on Dynamic Response of Offshore Wind Tower Founded on Monopoles." *International Conference on Mechanics and Civil Engineering, ICMCE 2014*, 305-310.
- Van Buren, E, and Muskulusa, M (2012). "Improving Pile Foundation Models for Use in Bottom-Fixed Offshore Wind Turbine Applications." *Energy Procedia*, 24, 363-370.